Molecular Crystals and Liquid Crystals

Publication details, including instructions for authors and subscription information:
http://www.tandfonline.com/loi/gmcl20

Thermal Behavior of Even Chain Length Lithium n-Alkanoates

Nicole A. S. White [a] & Henry A. Ellis [a]

[a] Department of Chemistry, University of the West Indies, Mona Campus, Jamaica

Version of record first published: 18 Mar 2009

To cite this article: Nicole A. S. White & Henry A. Ellis (2009): Thermal Behavior of Even Chain Length Lithium n-Alkanoates, Molecular Crystals and Liquid Crystals, 501:1, 28-42

To link to this article: http://dx.doi.org/10.1080/15421400802697202

Mol. Cryst. Liq. Cryst., Vol. 501, pp. 28–42, 2009

ISSN: 1542-1406 print/1563-5287 online
DOI: 10.1080/15421400802697202

Taylor & Francis
Taylor & Francis Group

Thermal Behavior of Even Chain Length Lithium n-Alkanoates

Nicole A. S. White and Henry A. Ellis
Department of Chemistry, University of the West Indies,
Mona Campus, Jamaica

The thermal phase sequences and thermal histories of a homologous series of even chain length lithium n-alkanoate, $LiC_nH_{2n-1}O_2$ (LiC_{8-18}), have been determined by differential scanning calorimetry. The phase changes accompanying heating these compounds above the melt are dependent on chain length. One intermediate phase is observed between the lamellar crystal and isotropic melt in the phase sequence for LiC_{10-12}:

$$lamellar\ crystal\ I \leftrightarrow lamellar\ crystal\ II \leftrightarrow isotropic\ liquid,$$

and two for LiC_{14-18}:

$$lamellar\ crystal\ I \leftrightarrow lamellar\ crystal\ II \leftrightarrow plastic\ crystal \leftrightarrow isotropic\ liquid.$$

*All the phase sequences are enantiotropic. Additionally, cooling and reheating runs are in good agreement with those of fresh samples. The premelting transitions, in the long chain length compounds, are preceded by an exothermic peak on heating fresh samples. This transition disappears on cooling and reheating the samples. It is probably due to the physical state of the melt in contact with the sample holder or from molecular structure factors, and not a liquid crystalline phase as proposed by an earlier study. The premelting transitions, in the long chain compounds, are ascribed to rotation of the methylene groups, in the crystalline lattice, resulting in a change in conformation from the nearly all-*trans *the more disordered plastic crystal phase, which is stable over a narrow temperature range. The thermodynamic data indicate that the melting processes are different for short and long chain adducts arising from subtle changes in their molecular structures.*

Keywords: differential scanning calorimetry; lithium n-alkanoates; x-ray powder diffraction

Address correspondence to Henry A. Ellis, Department of Chemistry, University of the West Indies, Mona Campus, Jamaica. E-mail: henry.ellis@uwimona.edu.jm

INTRODUCTION

The study of ionic liquids as solvents for organic, inorganic, and polymeric materials is of considerable interest, especially in the relatively new field of green chemistry. Long chain metal carboxylates form ionic melts that are easy to prepare, relatively inexpensive, and environmentally friendly [1–3]. It should be of interest, therefore, to study the thermal behavior of these materials.

Lithium carboxylates, like most monovalent metal soaps, pass through several intermediate phases as they are heated from the room temperature solid to the isotropic melt [4–7]. However, there are many disagreements concerning the number of phase transitions observed and their classification. This has arisen, principally, from variations in preparative and purification methods and in some cases, the presence of polymorphic structures [8]. For example, it has been suggested that a liquid crystalline phase is present on heating lithium palmitate [9] though subsequent studies [8,10] have suggested that those results were in error because of impure or possibly non-anhydrous starting materials. Moreover, no attempt has been made to correlate the phase sequences observed with chain length and molecular structures and the possible differences in molecular lattice arrangements that may arise from the change in chain lengths. Recent studies [10] have indicated that the molecular structures of the white paracrystalline solids were similar, at room temperature, with only slight differences in asymmetry around the lithium ion and in the packing of the hydrocarbon chains in the lattice. The hydrocarbon chains were located within a lamella as a bilayer, oriented tail-to-tail and tilted with respect to the lithium ion basal planes. The compounds crystallized within a triclinic unit cell with P1 or $P\bar{1}$ symmetry. Additionally, for the longer chain adducts, there was evidence for side chain interactions between hydrocarbon chains in the lattice suggesting a possible difference in how the hydrocarbon chains were packed within the crystal lattice.

In this study, the effects of variation in chain length and hydrocarbon chain packing in the crystal lattice on the thermal behavior of a homologous series of even-chain length lithium n-alkanoate, from octanoate to octadecanoate, inclusive ($LiC_{8\text{-}18}$), are investigated by differential scanning calorimetry (DSC) and X-ray powder diffraction in conjunction with polarizing light microscopy.

EXPERIMENTAL

The preparation and purification of the white microcrystalline solids have been reported in a previous article [10]. Their purity was checked

by elemental analyses using a Perkin Elmer Series II CHNSO Analyzer and by infrared analyses of samples recorded in KBr pellets on a Perkin Elmer FT-IR 1000 spectrophotometer, at room temperature, in the range of 4000–450 cm^{-1}. Melting points were determined, in duplicate, on a uni-melt Thomas Hoover melting point apparatus and also by DSC using a Mettler TC10A Processor connected to a DSC 20 cell. In a typical run a sample, weighing between 3–10 mg, was packed in a standard aluminum crucible and subjected to a heating–cooling–reheating cycle between 303–823 K at a rate of 2 K/min.

X-ray powder diffraction patterns were collected using a Bruker D5005 diffractometer with nickel filtered Cu-K_α radiation ($\lambda = 1.54056$ Å), at ambient temperatures, from finely ground samples mounted in standard plastic holders. The instrument was operated at 45 kV and 35 mA for an approximate run time of 3 hrs over a diffraction angle, 2θ, in the range of 2.5–50° at a step size of 0.02°, and a step time of 5 s. The data obtained were sorted for indexing and refined using BRUKER diffracAT evaluation program, part of the machine operating system.

RESULTS AND DISCUSSION

The elemental analyses data are given in Table 1 and are in reasonably good agreement with expected values. Also, the infrared traces are as expected for these compounds [10]. The melting point data, obtained visually and by DSC, along with the available literature data, are presented in Table 2. In the DSC method, the highest temperature endothermic transition is taken as the melting point. Those data are consistently higher than the visual and literature values, especially for soaps with the number of carbon atoms, $n_C > 12$. This can be attributed to differences in methods of preparation, thermal histories, presence of impurities, or more usually, mistaking a high temperature

TABLE 1 Elemental Anayses Data for LiC_n

Compound	% C	% H
LiC_8	63.36 (63.99)	9.98 (10.07)
LiC_{10}	67.34 (67.40)	10.79 (10.75)
LiC_{12}	69.34 (69.88)	11.13 (11.24)
LiC_{14}	70.89 (71.77)	11.40 (11.62)
LiC_{16}	72.27 (73.25)	11.76 (11.91)
LiC_{18}	74.09 (74.44)	12.08 (12.15)

Calculated values in parenthesis.

TABLE 2 Melting Point Data for LiC_n

Compound	Visual/°C	DSC/°C	Literature/°C [35]
LiC_8	259–260	264.3	+
LiC_{10}	241–242	244.0	+
LiC_{12}	226–227	228.4	229.2–229.8
LiC_{14}	220–221	229.7	223.6–224.2
LiC_{16}	193–196	228.8	224–225
LiC_{18}	216–217	227.0	220.5–221.5

+ - No available data.

phase, in the visual method, for the melting point [11,12]. Since impurities generally depress melting points, the DSC data collected here are considered to be more accurate and will be used subsequently. The short-chain length soaps melt at a higher temperature than their long-chain counter parts suggesting a possible relationship between melting point and chain length. Indeed, an almost exponential decrease in melting point is observed with increasing chain length. This may, in part, be ascribed to a difference in intramolecular attraction between adjacent hydrocarbon chains in competition with metal-carboxylate bonding. It is expected that metal-carboxylate bonding will predominate for short-chain length compounds over van der Waals interactions between chains, which is expected to be more predominant at higher chain lengths. Also, the change in the inductive effect of the carboxylate group along the chain and its increased floppiness with increasing chain length may also be contributory factors. These results are typical for alkali metal soaps and suggest that the compounds have considerable ionic character [13,14].

DSC curves for $LiC_{8\text{-}18}$ inclusive, in the temperature range of 303–823 K are shown in Fig. 1a. In a typical run, the sample is first heated to the isotropic liquid, cooled to room temperature, and then reheated, all at a constant rate of 2°C min^{-1}. On the first heating, one or more first order endothermic phase transitions are observed, the numbers of which increase with increasing chain length. For example, for $LiC_{10\text{-}12}$, inclusive, only one intermediate phase is observed between the lamellar crystal [10] and the isotropic liquid. In the case of $LiC_{12\text{-}18}$, inclusive, a pre-melting transition is always observed. This first appears as a very small shoulder on the melting transition of LiC_{12} and is gradually enhanced as chain length increases. Additionally, the transition and preceding small exothermic transition get progressively farther from the melting endotherm with increasing chain length. Although Ferloni and Westrum [7] reported a transition for LiC_8 at ca. 210 K, it is not seen here because our studies

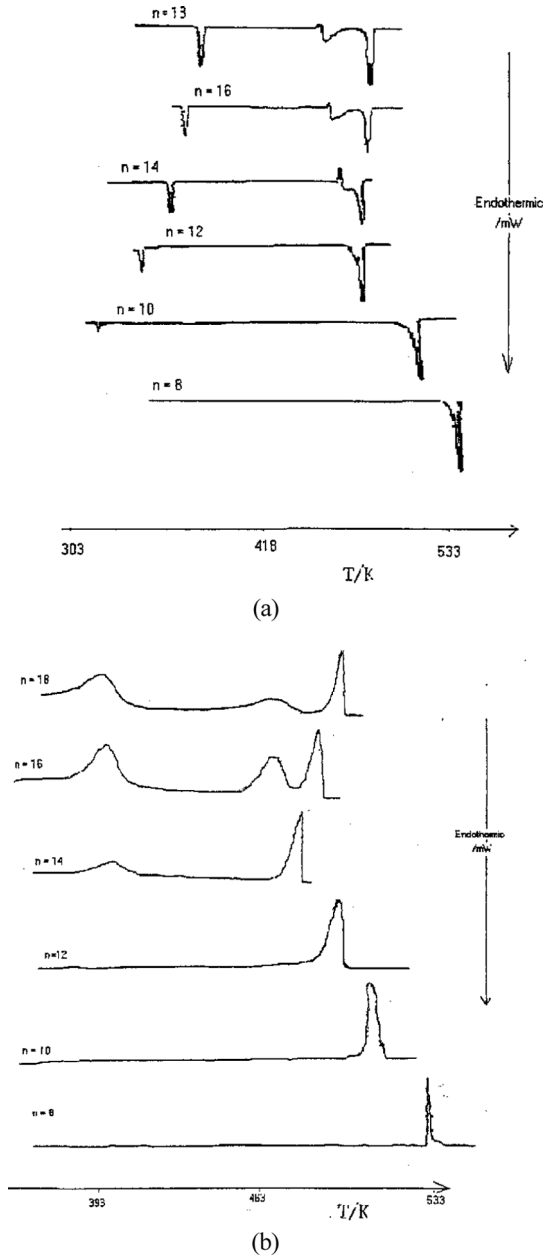

FIGURE 1 (a) DSC heating curves for LiC_n. (b) DSC cooling curves for LiC_n.

are limited to phase transitions between ambient and melting temperatures. The endothermic transitions observed in the region of 350–400 K are assigned as the lamellar crystal → phase 1, and the high temperature transition in the region of 501–525 K: phase 1 → isotropic melt. Additionally, the three endothermic transitions observed for $n_C > 14$ are designated as the lamellar crystal → phase I → phase II → Isotropic melt. Gallot and Skoulios [9], on the basis of X-ray powder diffraction, reported an additional transition for $LiC_{14\text{-}18}$ between phase I at 463 K and phase II at 496 K. This was suggested to be one of two ribbon phases. However, those transitions are not observed in this study, as well as in those reported by other studies [5,8,15]. The discrepancies may arise from impure starting materials, different preparative methods resulting in polymorphic forms of the starting material.

Because it is not possible to identify phase structures from these observations alone, cooling runs are performed to ascertain which transitions are liquid crystalline, where supercooling is expected to be minimal, or crystal to crystal when it is quite marked. These curves are shown as exotherms in Fig. 1b. They clearly show that the transitions are enantiotropic in contravention to the results reported by Vold and coworkers [8] where reversibility of phase transition was reported only for the lamellar crystal → phase I transition for LiC_{16}. Furthermore, supercooling is observed in all transitions, averaging between 5.77–19.50 K. This is strong evidence for crystal to crystal transitions. Further supporting evidence for this is provided by the resistance to a shear stress applied to the various phases sandwiched between slide and coverslip. That is, the phases are not mobile, as expected for a crystalline phase. Furthermore, on cooling into the low temperature phase, typical crystalline structures are observed (Fig. 2). Unfortunately, the results from cooling into the high-temperature phases, from the isotropic liquid, are inconclusive because the compounds change to a dark brown color at these elevated temperatures which make identification of phase structures impossible. A further observation is the gradual loss of birefringence on heating into the high-temperature phases.

The small exotherm that precedes the high temperature transition, for $n_C \geq 12$, is absent when the sample is cooled and reheated. These transitions are ascribed to the physical state of the melt, when on the first heating, the partially molten sample makes reasonable contact with the sample holder because of its lower viscosity. Thus, the transition is lost on reheating. This is clear evidence that it is not a true phase transition as reported earlier [8]. Also, molecular packing factors such as increased van der Waals interactions between

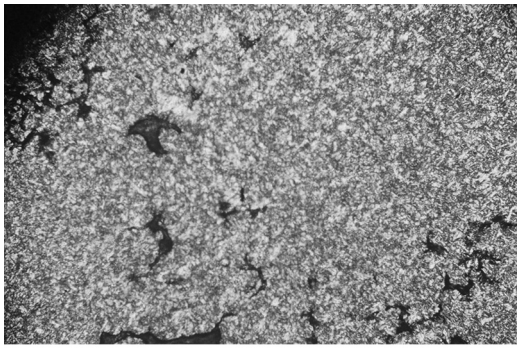

(a)

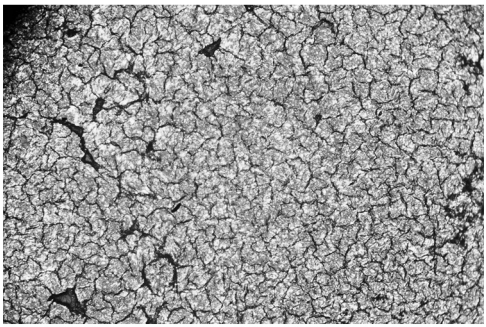

(b)

FIGURE 2 (a) Texture of LiC_{10} crystalline phase at 428.15 K, mag. × 10. (b) Texture of LiC_{10} crystalline phase at 303.15 K, mag. × 10.

hydrocarbon chains, at higher chain lengths, might also be a contributory factor. Indeed, similar transitions have been observed for other long and short chain metal carboxylates [16–19]. For example, the exothermic transitions reported for lithium formate and acetate (LiC_1 and LiC_2) have been suggested to be caused by a glass transition, observed when there is a change in heat capacity due to a decrease in viscosity in the samples [19,20].

Though the heating curves for the fresh and reheated samples are fairly similar, one obvious difference is the absence of the solid → phase 1 endothermic peak for LiC_{10} and LiC_{12} on reheating. These transitions are most probably metastable or kinetically controlled. It is also possible that melting and cooling the samples may result in the formation of polymorphic structures at room temperature as suggested by Burrows et al. [21,22] for other long chain metal carboxylates.

TABLE 3 Thermodynamic Data for Phase Changes

	T/K			$\Delta H \pm 0.54/Jmol^{-1}$		$\Delta S \pm 1.2/JK^{-}mol^{-1}$	
LiC_n	Heating	Cooling	Reheating	Heating	Reheating	Heating	Reheating
Crystal → phase 1							
LiC_{10}	314.40	*	*	3.00	*	9.53	*
LiC_{12}	349.40	*	*	5.42	*	15.51	*
LiC_{14}	369.53	410.00	363.10	8.34	1.93	22.56	5.30
LiC_{16}	382.27	404.00	378.50	10.44	7.63	27.31	20.16
LiC_{18}	392.20	401.00	387.70	13.53	8.32	34.51	21.45
Phase 1 → phase 2							
LiC_{14}	*	*	484.90	*	6.11	*	12.60
LiC_{16}	479.45	471.00	470.90	13.58	8.57	28.32	18.21
LiC_{18}	471.90	467.00	463.30	16.05	13.00	34.01	28.03
Phase 2 → isotropic liquid							
LiC_{14}	~501.2	*	502.10	*	13.88	*	27.67
LiC_{16}	501.77	489.00	500.00	17.34	14.21	34.56	28.43
LiC_{18}	500.00	491.00	499.70	17.30	16.56	34.60	33.14
Phase 1 → isotropic liquid							
LiC_{10}	517.00	*	*	22.88	*	44.26	*
LiC_{12}	501.40	*	*	27.97	*	55.78	*
LiC_{14}	502.70	489.00	*	36.79	*	73.19	*
Crystal → isotropic liquid							
LiC_8	537.50	530.00	536.70	23.02	23.80	42.85	44.34

*-No transition observed.

Phase transition data from heating–cooling–reheating the samples are collected in Table 3. The enthalpy, $\Delta_{trans}H$ and entropy, $\Delta_{trans}S$ data are only slightly different from those obtained on second heating. Plots of $\Delta_{trans}H$ and $\Delta_{trans}S$ for the lamellar crystal $\rightarrow$ phase I transition are shown as linear functions of n_C in Fig. 3. This indicates that melting, up to this point, is a stepwise process for all homologues. On extrapolating the graph, negative entropies are obtained for the lower chain length compounds indicating no sharp crystal $\rightarrow$ crystal transition are to be expected for these compounds as is observed. For the phase I $\rightarrow$ phase II transitions, there is no discernable relationship between $\Delta_{trans}H$ and $n_{C.}$ However, the enthalpy values, for the transition, do not vary much suggesting some similarity in structures between phases I and II. Moreover, the overall enthalpy changes associated with the fusion of these compounds, $\Delta_{fus}H$ show a gradual increase with chain length up to $n_C = 12$, followed by a sharp drop to a fairly constant value. This clearly suggests that homologues with chain lengths $n_C \leq 12$ undergo a similar melting process. For the longer chain length adducts, the near linear relationship between $\Delta_{fus}H$ and $\Delta_{fus}S$ versus n_C suggests that melting is strongly chain-length dependent, and a different fusion mechanism is in operation for them. Ferloni and Westrum [7] proposed a similar dual mechanism for long and short chain-length lithium carboxylates. Additionally, the slope of $\Delta_{total}H$ versus n_C is 2.54 kJ (mol CH_2)$^{-1}$, somewhat less than the expected value of 3.8 kJ (mol CH_2)$^{-1}$ [23] for complete fusion of

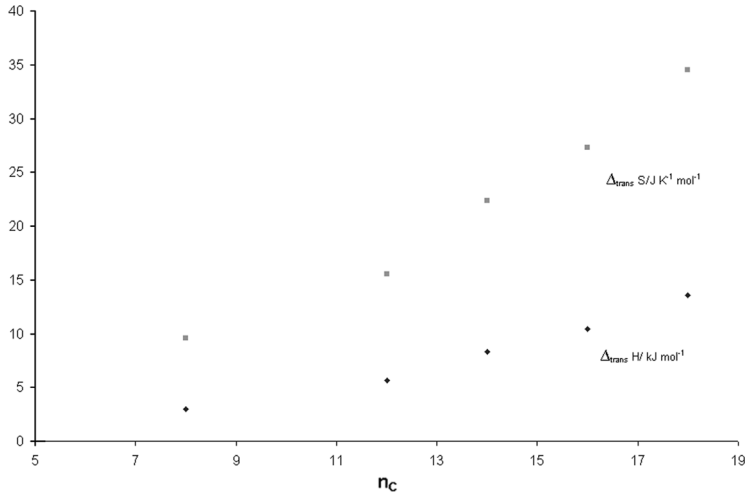

FIGURE 3 Enthalpies and entropies of phase transitions versus chain length.

hydrocarbon chains from the room temperature crystalline phase to the melt. Also, the slope of $\Delta_{total}S$ versus n_C of 6.21 is smaller than the expected value of 10 JK^{-1} (mol $CH_2)^{-1}$ for complete fusion [24]. Therefore, melting occurs without complete fusion of hydrocarbon chains, and hence some crystalline order is maintained in the melt. Sime and co-workers [25] have suggested, from electrical conductivity studies, that the melts in long chain lead soaps contain areas of ordered micelles, though is unclear whether these structures are present here. Clearly, the melting behavior of these might not only be chain length dependent, but could also be due in part to changes in the molecular crystal lattice between short and long chains. One approach is to use X-ray diffraction studies to ascertain whether there are any differences in the molecular lattice structures of the room-temperature starting materials.

Because at present it is not possible to prepare single crystals for X-ray studies, X-ray powder diffraction studies are performed on all the homologues. Thus, representative X-ray powder diffraction patterns, at room temperature, for LiC_8 and LiC_{16} are shown in Fig. 4 as intensity of the diffracted ray, I versus angle of diffracted ray, 2θ. Generally, all compound exhibit evenly spaced reflections at low Bragg angles. Their regularity indicates diffraction from an ordered structure generally agreed to be laminar [10,26–28]. However, for the longer chain length homologues ($n_C > 12$) the pattern changes somewhat in the region of $20^\circ \leq 2\theta \geq 25^\circ$, where closely spaced low-intensity reflections are observed. This region is associated with side chain packing for disordered chains [10,29] and their absence in the shorter chain adducts suggests that short and long chain are not similarly packed within the crystal lattice. Indeed, these side chain interactions indicate a higher degree of *gauche* conformations in the longer chain adducts and indicate some subtle change in packing of the hydrocarbon chains in the lattice with increasing chain length which may result in the different phase transition sequences observed for the long and short chains.

Commercially available Win-metric LS software for windows was used to analyze the X-ray data. Details of the analyses are given elsewhere [10]. Those results indicated that the compounds crystallized along side c as the principal axis, that being the side that showed the greatest increase with successive additions of methylene groups to the chain. Furthermore, the near linear line obtained for the plot of c versus n_C($R^2 = 0.84$), confirms that the homologues are fairly similar in structure, though there is some indication that the lower homologues, $n_C = 8$, 10, are not such a good fit. This clearly supports the notion of a subtle difference in molecular packing between short and long chains. Indeed, Lomer and Perera [30] showed that hydrocarbon

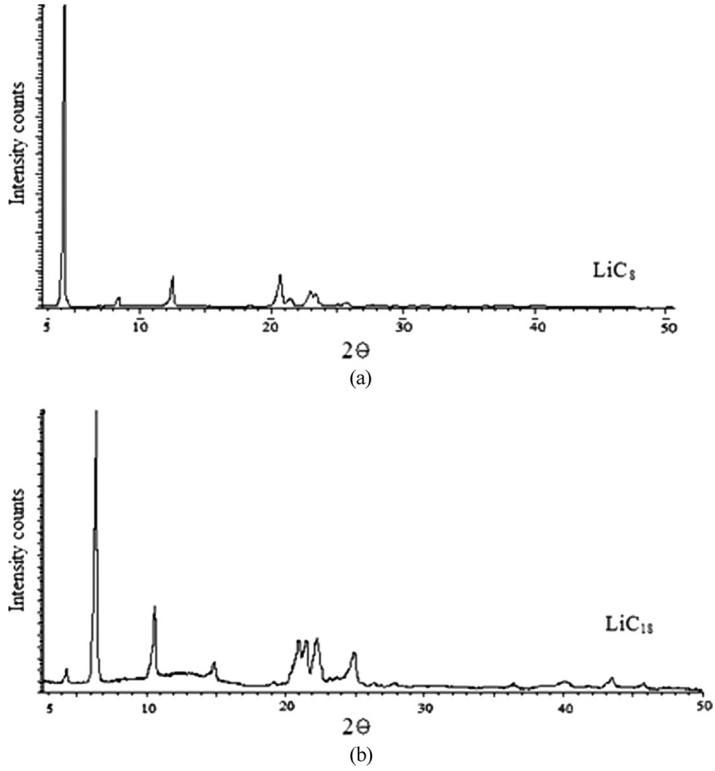

FIGURE 4 X-ray powder diffraction patterns for LiC_8 and LiC_{16}.

chains did not pack into the crystal lattice in the same way even in going from copper (II) octanoate to decanoate.

Lamellar spacings (d_{exp}) obtained from 001 reflection for each compound are compared with molecular lengths (d_{cal}), assuming that the alkyl chains are arranged, nearly, in the all-*trans* conformation [10]. An analysis of the data in Table 4 shows d_{cal} is a little more than half the observed lamellar spacing. This is interpreted to mean that the molecules are arranged as bilayers within a lamella and tilted at an average angle of $\sim 55^\circ$ to the plane containing the metal ion. Conoscopic studies carried out on LiC_{10} confirm the tilted arrangement of chains; that is, the expected biaxial interference figure is observed. Indeed, the evidence for molecular tilting in similar long chain compounds is overwhelming [22,31,32].

Because cooling into phase1 is accompanied by supercooling, in conjunction with the phase not being fluid, indicates that this is a

TABLE 4 d_{exp} from 001 Plane and d_{cal} for LiC_n

Compound	d_{exp}/Å	$2d_{cal}$ /Å
LiC_8	21.05	24.12
LiC_{10}	24.51	29.16
LiC_{12}	28.21	34.22
LiC_{14}	33.69	39.26
LiC_{16}	37.30	44.30
LiC_{18}	41.90 [36]	49.36

crystalline phase. Moreover, the small increase in enthalpy and entropy on heating into the phase suggests that the lamellar structure is minimally altered in phase1. Indeed, X-ray studies [9] suggest that phase1 differs from the room-temperature crystal by a change in the tilt angle of the hydrocarbon chains and is, therefore, identified as a lamellar II crystal phase. However, the high temperature phase has been variously described as a ribbon or plastic phase [8,9,33]. The $\Delta_{trans}H$ and $\Delta_{trans}S$ values suggest a greater change in orientation than a change in tilt angle, and hence it is unlikely to be a lamellar crystal phase. Indeed, Gallot and Skoulios [9] reported a halo at 4.5 Å, in the X-ray powder photograph for LiC_{16}, as a sign of the disorientation of the hydrocarbon chains, and a group of 10–20 distinct lines in the central region of the photograph as representative of a bidimensional rectangular center consisting of the carboxylate group. Clearly, there is a change in conformational order in the hydrocarbon chains, from the nearly all-*trans* to *gauche* conformation. That is, the chains rotate, on being heated, and free methyl groups interact with neighbouring chains forcing them to rotate as well thus effecting the change to *gauche* conformation [34]. The effect is enhanced, progressively, on heating. Therefore, the loss of orientation in the hydrocarbon chain and retention of some positional order in the carboxylate group is indicative of a plastic crystal. The melting transitions for the entire series, whether from crystal II → isotropic liquid or plastic crystal → isotropic liquid, is chain length dependent.

A plot of phase transition temperatures versus n_C is shown in Fig. 5. Connecting curves are drawn on the basis of the few optical textures observed on cooling into the various phases and DSC data. The plastic crystal phase appears only for long chain length adducts and is stable over a narrow temperature range. The lamellar crystal II phase is stable over a wide chain length and temperature range, and is structurally different from the lamellar crystal I phase. This difference is attributed to a change in tilt angle of the hydrocarbon chain with respect to the lithium ion basal plane.

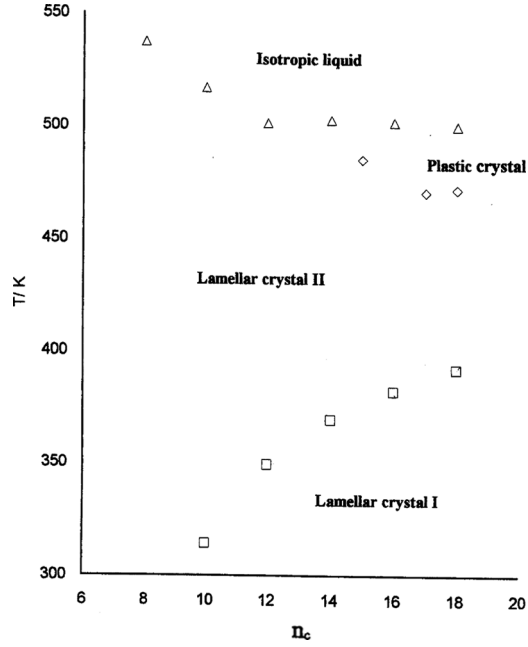

FIGURE 5 Phase transition temperature versus chain length.

CONCLUSION

An even-numbered series of solid lithium carboxylates are studied by DSC, from room temperature to just above the melt, and by X-ray powder diffraction at room temperature. The numbers of first order transitions are dependent on chain length. For the short-chain length compounds, the phase sequence: lamellar crystal I $\leftrightarrow$ crystal II $\leftrightarrow$ isotropic melt is suggested. For the long chain length adducts a plastic crystal is observed between the lamellar II crystal to isotropic melt. An additional premelting endotherm, preceded by a small exotherm, is observed for chain lengths, $n_C \geq 12$. This endotherm is better resolved on reheating and is ascribed to the rocking of methylene groups, in the crystal lattice, as the alkyl chains move from the nearly all-*trans* conformation to a more disordered plastic crystal. Since the exotherm disappears on cooling and reheating the sample, it probably results from the physical state of the melt in contact with the sample holder, and on molecular packing factors, and not a liquid crystalline phase as reported elsewhere. The melting processes in the long and short chains are different, arising from a subtle change in their molecular lattices at room temperature. All the phases are stable over a wide

temperature range, except the plastic phase which is present only in the phase sequence for long chain length compounds.

REFERENCES

[1] Wilkes, J. S. (2002). *Green Chem.*, *4*(2), 73.
[2] Seddon, K. R. (1998). Molten Salt Forum: Proceedings of 5th International Conference on Molten Salt Chemistry and Technology, H. Wendt (Ed.), 5–6, 53.
[3] Welton, T. (1999). *Chem. Rev.*, *99*, 2071.
[4] Vold, M. J., Macomber, M., & Vold, R. D. (1941). *J. Amer. Chem. Soc.*, *63*, 168.
[5] Vold, R. D., & Vold, M. J. (1941). *J. Phys. Chem.*, *49*, 32.
[6] Lee, S. J., Han, S. W., Choi, H. J., & Kim, K. (2002). *J. Phys. Chem. B*, *106*, 2892.
[7] Ferloni, P., & Westrum, Jr., E. F. (1992). *J. Pure and Appl. Chem.*, *64*(1), 73.
[8] Vold, M. J., Funakoshi, H., & Vold, R. D. (1976). *J. Phys. Chem.*, *80*(15), 1753.
[9] Gallot, B., & Skoulios, A. (1966). *Kollid-Zeitschrift fur Polymere Band*, *209* (Heft 2), 164.
[10] White, N. A. S., & Ellis, H. A. (2008). *J. Mol. Str.,* in press.
[11] Bancroft, D. P., Cotton, F. A., Falvello, L. R., & Schwotzer, W. (1988). *Polyhedron*, *7*, 615.
[12] Markley, K. S. (1961). *The Fatty Acids* (2nd Ed.), Chapter 8, Interscience: New York.
[13] Adeosun, S. O., & Ellis, H. A. (1979). *Thermochim. Acta*, *28*, 313.
[14] Phillips, M. L., & Jonas, J. (1987). *Liq. Cryst.*, *2*, 335.
[15] Benton, D. P., Howe, P. G., & Puddington, I. E. (1955). *Can. J. Chem.*, *33*, 1384.
[16] Ellis, H. A. (1986). *Mol. Cryst. Liq. Cryst.*, *138*, 321.
[17] Barr, M. R., Dunnel, B. A., & Grant, R. F. (1963). *Can. J. Chem.*, *41*, 1188.
[18] Berchiesi, G., Berchiesi, M. A., Lobbia, G. G., & Leonesi, D. (1976). *Gazzetta Chimica Italiana*, *106*(3–6), 549.
[19] Tanford, C. (1973). *The Thermodynamic Effect: Formation of Micelles and Biological Membranes*, Wiley: New York.
[20] Skoog, D. A., Holler, F. A., & Nieman, T. (1998). *Principles of Instrumental Analysis* (5th Ed.) Harcourt Brace Jovanovich, New York.
[21] Burrows, H. D. (1990). *The Structure, Dynamics of Equilibrium Properties of Colloidal Systems*, Bloor, D. M. & Wyn-Jones, E. (Eds.), Kluwer: Dordrecht, 415.
[22] Ellis, H. A., White, N. A. S., Taylor, R. A., & Maragh, P. T. (2005). *J. Mol. Str.*, *738*, 205.
[23] Seurin, P., Guillon, D., & Skoulios, A. (1881). *Mol. Cryst. Liq. Cryst.*, *65*, 85.
[24] Marques, E. F., Burrows, H. D., & daGraca Miguel, M. (1998). *J. Chem. Soc. Faraday Trans.*, *94*(12), 1729.
[25] Ekwunife, M. E., Nwachukwu, M. U., Rinehart, F. P., & Sime, S. J. (1975). *J. Chem. Soc., Faraday Trans., 1*, 1432.
[26] Wong, P. T. T., & Mantsch, H. H. (1983). *J. Phys. Chem.*, *87*, 2436.
[27] Ubbelohde, A. R. (1968). *Chem. & Ind.*, *311*, 313.
[28] Haseda, T., Yamakawa, H., Ishizuka, M., Okuda, Y., Kubota, T., Hata, M., & Amaya, K. (1977). *Solid State Comm.*, *24*, 1599.
[29] Corkery, R. W. (2004). *Phys. Chem. Chem. Phys.*, *6*, 534.
[30] Lomer, T. R., & Perera, K. (1974). *Acta Cryst.*, *B30*, 2913.
[31] Ellis, H. A., White, N. A. S., Hassan, I., & Ahmad, R. (2002). *J. Mol. Str.*, *642*, 71.
[32] Ellis, H. A. (1986). *Mol. Cryst. Liq. Cryst.*, *139*, 281.

[33] Skoda, W. (1969). *Kolloid-Zeitschrift und Zetschrift fur Polymere Band 234 (Heft 2)*, 1128.
[34] Nagle, J. F. (1980). *Ann. Rev. Phys. Chem.*, *31*, 157.
[35] Lide, D. E. (1981). (Ed.). *Handbook of Chemistry and Physics,* 62nd Ed., p. F-5, CRC Publishing Company, Cleveland, OH, USA.
[36] Shoeb, Z. E., Hammad, S. M., & Yuosef, A. A. (1999). *Grasas Y Aceites*, *50*(6), 426.